Synthesis of plant-mediated silver nanoparticles using Veronica anagallis-aquatica extract; Optical and biological properties

Mushtaq Ahmed (mushtaq213@yahoo.com)
University of Science and Technology Bannu https://orcid.org/0000-0002-0286-326X
Aman Khan
Nadia Mushtaq
Naila Sher
Rahmat Ali Khan

Research Article

Keywords: Veronica anagallis-aquatica, AgNPs synthesis, characterization

Posted Date: June 8th, 2022

DOI: https://doi.org/10.21203/rs.3.rs-1642963/v1

Abstract

There is an increasing commercial demand for nanoparticles due to their wide applicability in various areas such as electronics, catalysis, chemistry, energy, and medicine. Metallic NPs are traditionally synthesized by wet chemical techniques, where the chemicals used are quite often toxic and flammable. The focus of the current study was the green synthesis of silver nanoparticles (AgNPs) from 1 mM silver nitrate ($AgNO_3$) solution using an aqueous solution of *Veronica anagallis-aquatica* (*V. anagallis-aquatica)*. Fixed ratio of $AgNO_3$ and plant extract was mixed and conformation of AgNPs was done by UV visible spectroscopy; which showed a maximum absorption peak at 425 nm. The Fourier transformed spectroscopy (FTIR) spectrum shows various peaks for different functional groups bearing compounds that had played role in the bioreduction of AgNPs. Scanning electron microscopy (SEM) analysis demonstrated that AgNPs were spherical with a size of about 20 nm calculated by Nano measurer software. The average size of 11.45 nm was calculated using four major peaks 38°, 44°, 64°, and 78° of X-rays diffraction (XRD) analysis. The chemical composition of AgNPs was revealed by Energy dispersive X-ray (EDX). The atomic and weight percentages of Ag, Na, Mg, and O were 73.55, 17.91, 6.78, 1.75, and 60.58, 21.20, 8.49, and 9.74. EDX confirmed the intense sharp peak at 73.55 keV. The in vitro antioxidant, antibacterial, antifungal, antidiabetic, and TBARS were found with positive results. The current study concluded that *V. anagallis-aquatica* possesses the ability to synthesize AgNPs. These synthesized AgNPs showed enhanced properties compared to the *V. anagallis-aquatica.*

1 Introduction

In several fields, medical, food, industry, etc, the silver nanoparticles (AgNPs) emergence is observed significantly high in the last few years [1]. This is because AgNPs exhibit unique chemical and physical properties. These properties range from electrical to biological properties [2]. AgNPs are also used in textile industries, keyboard preparation, and wound healing [3]. AgNPs have been used in the research and development field for the enhancement of their intrinsic characteristics [4]. Silver is supposed to be a non-toxic and safe antimicrobial agent having the capability of killing around 650 numerous types of microorganisms. The researcher's interest has grown significantly in recent years to use AgNPs as antimicrobial agents [5]. The mechanism through which their synthesis takes place is yet to be explained [6]. Various scientific parameters might be used in the biosynthesis of AgNPs [7]. The biological actions of AgNPs are dependent upon various factors including shape, size, surface chemistry, size distribution, composition and morphology, dissolution rate, the efficiency of cells and ions produced in their reactivity, the type of reducing agents, etc. The AgNPs hold their importance in various biomedical applications because the bioavailability of the therapeutic agents, after local and systemic administration, is improved many folds by the AgNPs. Apart from that, AgNPs may also increase the biological distribution of the therapeutic agents, their cellular uptake in the body, their diffusion into various barriers, and their healing properties. Therefore, the synthesis of AgNPs with their controlled structure is imperative in numerous biomedical uses [8–10]. Various methods or strategies are adopted for the synthesis of AgNPs. Some are briefly described here. Laser ablation and evaporation condensation are various physical approaches to

the synthesis of AgNPs. Metal nanoparticles (NPs) including gold, silver, lead, and cadmium have been synthesized [11]. Chemical reduction with the help of reducing inorganic and organic compounds like sodium borohydride, sodium citrate, and ascorbate is used as reducers for the chemical synthesis of AgNPs [12]. Synthesizing AgNPs using green chemistry, in which naturally occurring reducing, stabilizing, and capping agents are utilized. The method is favored over physical and chemical methods because of having no toxic effects on the AgNPs and is cheap [13]. Silver or metal-based synthesized NPs possess effective biological properties [14].

Veronica anagallis-aquatica (*V. anagallis-aquatica*) belongs to the kingdom Plantae (Angiosperms), Order Lamiales, Family Plantaginaceae, Genus Veronica, and Species anagallis-aquatica. It is also known as water speedwell and blue speedwell. It is a perennial herb with a stem similar to a root and horizontal in position and is mostly found in moist habitats. The true native land of this plant is not known but it is present all over the world. Its stem can reach a maximum of 10 centimeters to about one meter in length.

To the best of our knowledge, *V. anagallis-aquatica*, the extract has not yet been tested for AgNPs synthesis. So in the present work, very stable AgNPs were synthesized using *V. anagallis-aquatica* extract. *V. anagallis-aquatica* extract acted both as a reducing as well as a capping agent. Antioxidant, antibacterial, antifungal, antidiabetic, and thiobarbituric acid activities of synthesized AgNPs were evaluated.

2 Materials And Methods

2.1 Collection, Identification, and Extraction of plant material

V. anagallis-aquatica collection was done from district Bannu Khyber Pakhtunkhwa (Surrani area), and was recognized by Dr. Faizan Ullah at the department of Botany, University of Science and Technology Bannu by a taxonomist. The leaves detached from the whole plant were washed using water to remove dust particles. The fresh cleaned leaves (2.5gm approximately) were taken in a 250 ml flask and added to 100 ml deionized water and boiled for 10 minutes to facilitate the formation of aqueous extract. Leaves were chopped into fine particles and then the mixture was kept for 24 hours in a laboratory at room temperature and further filtered using Whatman No.1 filter paper.

2.3 Silver nanoparticles synthesis (AgNPs)

For AgNPs synthesis according to the standard protocol of [15], 10 ml solution from10 mM silver nitrate solution was added to 1 ml aqueous leaves extract and incubated in the dark. The resulting solution was then analyzed using ultraviolet-visible spectroscopy. To be dried dry powder of silver nanoparticles, the solution was centrifuged at 13000 rpm for 2 minutes and was then washed with deionized water at least three times.

2.4 Factors affecting synthesis rate, size, and shape of AgNPs

To study the effect of *V. anagallis-aquatica* extract on the synthesis of AgNPs concentration of the *V. anagallis-aquatica* extract was varied from 0.5-2 ml. To study the effect of the temperature, AgNPs were synthesized at different temperatures 25°C, 50°C, 75°C, and 100°C. To study the effect of acidic and basic conditions on the synthesis of the AgNPs pH of the reaction mixture was maintained from 2-to 12 respectively. To study the effect of the time on the completion of the reaction was monitored from 0 to 30 min after every 5 min interval and the last reaction was monitored after 24 hrs [16].

2.5 Characterization of AgNPs

The reduction of the silver ion in the solution was determined using SHIMADZU UV SPECTROPHOTOMETER (UV-1800). The purified AgNPs were examined for the presence of the various functional groups using the FT-IR Shimadzu (IR Prestige-21) spectrometer (Japan). FT-IR analysis was carried out through Shimadzu (IR Prestige-21) spectrometer (Japan). The prepared materials were fully dried to remove the traces of moisture before subjecting them for FTIR analysis. Potassium bromide (KBr) powder was also dried 2–3 times. For blank analysis, a pure KBr pellet was prepared and used. Then 5% solid solution of each sample with KBr in the form of a thin pellet was prepared. The FT-IR spectra of the materials were obtained in the IR radiation range 500–4000 cm-1. The crystalline nature of the AgNPs was determined by JDX-3532 (JEOL JAPAN) X-ray diffractometer having a fixed radiation wavelength of λ-1.54 Aº. For structural analysis, the XRD patterns of the prepared materials were studied by JDX-3532 (JEOL JAPAN) X-ray diffractometer having a fixed radiation wavelength of λ-1.54 Aº. Each sample was sized to one square inch for XRD analysis. The samples were placed in a glass-made holding system and then transferred to the X-ray generating tube. The acceleration voltage of 35 kV and 20 mA current were applied while the degree of scanning was in the range from 10 to 50°. The diffracted intensities were recorded from 20° to 80°. The size and shape of NPs of the prepared materials in the project were analyzed by using JEOL SCANNING ELECTRON MICROSCOPE MODEL JSM-5910 (Japan). Current-voltage applied was in the range from 5 kV-20 kV. The resolution of the microscopic lens varied from 10000X to 50000X. An appropriate amount of samples were taken and mounted on Aluminum stubs with conductive taps and then subjected to SEM analysis. Micrograph images of all the samples were obtained under suitable resolution and voltage. The purity of AgNPs in solution was determined by using the EDX NOVA-450 instrument technique.

2.6 Biological Activities of AgNPs

2.6.1 Antibacterial activity

The antibacterial activity of the synthesized AgNPs was carried out using the agar well diffusion method [17]. Three bacterial strains (*E. coli, S. aureus, K. pneumoniae*) were used to assess the antibacterial activity. The concentration of 100, 500, and 1000 µg/ml of extract and AgNPs were used. Nutrient agar and all other material were sterilized. About 20 ml of nutrient growth medium was poured into Petri plates

and allowed them to cool at optimum temperature. The bacterial strains were streaked using a sterilized swab. Wells were punctured in the agar and 70 µl samples (both extract and AgNPs), dimethyl sulfoxide (DMSO) as a negative control, and standard drug (Levofloxacin) were administered into the wells, and plates were placed for a period of 24 hrs in a safety cabinet. At the end of 24 hrs, readings were taken as an inhibitory zone in mm.

2.6.2 Antifungal activity

The antifungal assay was performed using a standard protocol of [18]. Two fungal strains (*Aspergillus niger* and *Aspergillus flavus*) were used. The fungal media that was incorporated was saboroud dextrose agarose (SDA). 9 gm SDA was liquefied in 100 ml deionized water and autoclaved to get rid of contamination. About 10 ml of this SDA was poured into each test tube in a safety cabinet. Nearly 4 mm of fungal strains were detached from the parent culture and put into the respective test tube. About 200 µl extract, as well as AgNPs, were also poured into the tubes. Terbinafine served as a positive control; while DMSO served as a negative control. The readings were taken after 3 days.

2.6.3 Antioxidant Activity

2.6.3.1 DPPH assay

DPPH assay was performed according to [19]. About 0.003 gm of DPPH mixed in 50 ml of deionized H_2O. Ascorbic acid was used as standard. 200 µl from different concentrations of AgNPs and plant extract was mixed with 800 µl freshly prepared DPPH solution. After dark incubation of 30 min absorbance was measured against a blank at a wavelength of 517 nm using a BMS spectrophotometer. % scavenging was calculated by using the formula (i);

% scavenging = Ac-As/Acx100 (i)

Where Ac = Control absorbance, As AgNPs and plant extract absorbance

2.6.3.2 ABTS radicals scavenging activity

The standard method of [20] was used for ABTS radicals scavenging. 2.45 mM Potassium persulfate and 7 mM ABTS solutions were made in deionized H_2O. The two solutions were left for an overnight period after intermixing with one another. Production of a dark blue color confirmed the presence of ABTS free radicals. Optical density was measured using a spectrophotometer and adjusted to 0.7. About 300 µl AgNPs solution and plant extract were mixed with the same volume of ABTS solution and absorbance were taken at 734 nm. % scavenging was calculated by using the formula (i).

2.6.3.3 H_2O_2 radicals scavenging activity

The hydrogen peroxide (H_2O_2) assay was performed using the standard method [21]. About 200 µl AgNPs and plant solution, 400 µl H_2O_2 (2 mM) solution, and 400 µl phosphate buffer (50 mM) of 7.4 pH were

mixed; followed by 20 min incubation. Absorbance was measured at 617 nm using a BMS spectrophotometer against a blank. % scavenging was calculated by using the formula (i).

2.6.4 Antidiabetic activity (α-amylase activity)

The in vitro antidiabetic activity was assessed using the standard method [22]. About 200 µl α-amylase solution was mixed with equal volumes of various concentrations of the synthesized AgNPs and plant extract. This solution could incubate for 10 min at room temperature. After incubation, 200 µl starch solution was added to all the tubes and again incubated for three minutes. About 200 µl of dinitro salicylic acid was added to each test tube and heated for ten minutes at 95ºC. Nearly 5 ml of distilled water was added to the tubes after cooling time. The % inhibition was assessed by following the equation (i).

2.6.5 TBARS (Thiobarbituric acid reactive substances) assay

The lipid peroxidation produces a product, Thiobarbituric acid reactive substances e.g. malondialdehyde (MDA) assessed by TBARS assay. This assay measures malondialdehyde (MDA) present in the test sample. The standard method of [23] was used. Centrifugation at speed of 4,000 x g for 10 min was used for homogenate to yield a pellet and the supernatant. Pellet was unused and the supernatant was used. At 37°C, for 60 min 100 µl supernatant was incubated in the presence or absence of plant extract and AgNPs. After incubation, TBA, 8.1% SDS, and acetate buffer were added and again incubated for 60 min at 100°C. The formation of the light pink color showed the reaction of MDA with TBA. By using ice tubes were cooled, absorbance was measured at 532 nm.

3. Results

3.1 Synthesis of AgNPs

3.1.1 Ultraviolet visible technique

Silver nitrate ($AgNO_3$) solution turned black after the addition of plant extract which indicated the formation of AgNPs. The solution was checked by UV-visible spectroscopy at wavelengths between 200–800 nm. Figure 1 indicated 425 nm absorption bands of the AgNPs

3.1.2 Factors affecting the synthesis of silver nanoparticles

Various concentrate of ions 0.5-2 ml plant extract was used and absorbance was recorded in a UV-Visible spectrophotometer. Absorbance at 425, 425, 430, and 430 nm showed (Fig. 2a). The Surface Plasmon Resonance bands became sharper by increasing plant extract concentration and appeared at 430 (absorbance 0.99982) at a lower concentration of 0.5 ml and 425 nm (absorbance 1.6) at a higher concentration of 2 ml.

Different temperature conditions 25ºC, 50ºC, 75ºC, and 100ºC were used for AgNPs synthesis. Absorbance at 435, 430, 425, and 425 nm was recorded (Fig. 2b). At a lower temperature, a 25ºC absorbance peak of 425 (absorbance 1.75) was observed which increased with the increase in temperature, and a final absorbance peak of 435 nm (absorbance 2.401) was observed at 100 ºC.

Figure 2c shows AgNPs formation at different time intervals. Absorbance (1.279992) at 409 nm appeared after 5 minutes. This absorbance peak becomes sharp with the passage of time and a final 430 nm peak with the absorption of 2.1996 was recorded after 24 hours.

Figure 2d indicated the formation of AgNPs at different pH. An almost straight line was observed at acidic pH values of 1–6; while with an increase of pH the sharp peaks 420, 425, and 430 nm were recorded in pH range of 7–12.

3.2 Characterization of AgNPs

3.2.1 Analysis through Fourier Transformed Infrared (FTIR)

The FTIR technique was performed to identify the possible biomolecules with their different functional groups. Peaks at 3500 to 3100, 1725, and 1415 cm-1 relate to hydroxyl functional group in molecule and hydrogen bonds involving OH group, C = O groups, and Carbon double bond aromatic ring vibrations were shown by plant extract sample (Fig. 3a). AgNPs FT-IR demonstrates clear variation in the location of some peaks i.e. at 3500 to 3100, 1695, 1442, 1300, and 1000 cm-1 and they relate to OH group, C = O group, stretching C = C aromatic ring, and C-OH stretching vibrations. This determines the interaction between $AgNO_3$ and the functional groups that are involved sites of phytochemicals in reducing the salt (Fig. 3b).

3.2.2 Analysis through X-Ray D diffraction (XRD)

AgNPs' exact nature can be determined by the XRD spectrum. Distinct peaks of 38°, 44°, 64°, and 78° are recorded in a spectrum of values ranging from 20-to 80 (Fig. 4). Debye-Scherer's formula has been used for size evaluation.

D=

D = crystallite size (nm)

K = Scherer's constant = 0.9

λ = X-ray wavelength = 0.15406 nm

β = FWHM = Full length at half maximum (radian)

θ = Peak position (Radian)

Nanoparticles size was calculated by using the above-mentioned formula, which was 11.45 nm.

3.2.3 Scanning electron microscopy analysis (SEM)

SEM analysis clearly shows that the AgNPs are small and uniform in size, almost spherical in nature is free from agglomeration (Fig. 5). Using nano measurer software average particle size was calculated which is about 20 nm.

3.2.4 Energy-dispersive X-ray analysis (EDX)

The chemical composition of biologically synthesized AgNPs was revealed by the EDX spectrum. Different peaks strong peak from silver (Ag) and small peaks from Sodium (Na), Magnesium (Mg), and Oxygen (O) was observed in the spectrum. The atomic and weight percentages of Ag, Na, Mg, and O were 73.55, 17.91, 6.78, 1.75, and 60.58, 21.20, 8.49, 9.74 (Fig. 6).

3.3 Antibacterial and antifungal assay

The antifungal potential of plant extract and AgNPs were assed (Fig. 7). AgNPs showed good antifungal inhibition as compared to the plant extract. Results are mentioned in Table 1. AgNPs and plant extract antibacterial results are shown in Fig. 8. The results showed that AgNPs exhibited a higher zone of inhibition as compared to plant extract while lower as compared to the standard antibacterial drug (Table 2).

Table 1
AgNPs vs. *Veronica anagallis-aquatica* (VAA) extract inhibition against fungal strains

Species	Terbinafine	DMSO	DDH_2O	100 µg/ml	500 µg/ml	1000 µg/ml
A. niger (VAA)	130 mm	0	0	14 mm	20 mm	22 mm
A. niger (AgNPs)	130 mm	0	0	27 mm	50 mm	65 mm
A. flavas (VAA)	130 mm	0	0	09 mm	10 mm	11 mm
A. flavas (VAA)	130 mm	0	0	14 mm	28 mm	130 mm

Table 2
Zone of inhibition of *Veronica anagallis-aquatica* (VAA) extract and AgNPs against various bacterial strains

Zone of inhibition (mm)										
S. no	Strains									
		100 µg/mL		500 µg/mL		1000 µg/mL		Levofloxacin DMSO		
		VAA	AgNPs	VAA	AgNPs	VAA	AgNPs	AgNPs	VAA	
3	*E. coli*	0	8	1	9	3	10	20	18	0
5	*S. aureus*	0	8	1	10	3	11	16	15	0
6	*K. pneumonia*	0	5	1	6	2	7	18	20	0

3.4 Antioxidant assay

3.4.1 DPPH Activity

Synthesized AgNPs possessed commendable antioxidant activity as compared to the plant extract but showed lesser scavenging potential than the standard ascorbic acid (Fig. 9a).

3.4.2 ABTS activity

Our findings noted a significant ABTS antioxidant effect of synthesized AgNPs as compared to plant extract which showed the least activity. The ascorbic acid scavenging percentage was somewhat above the AgNPs (Fig. 9b).

3.4.3 Hydrogen peroxide assay

Different concentrations of AgNPs and plant extract (20–100 µg/ml) were tested against hydrogen peroxide free radicals to check AgNPs scavenging potential. The higher concentration of 100 µg/ml of ascorbic acid, AgNPs, and plant extract revealed 89.69%, 87.11%, and 53.8% percentage scavenging respectively (Fig. 9c).

3.4.4 Antidiabetic activity (Alpha amylase activity)

In vitro inhibitory effect of AgNPs against α-amylase enzyme is shown in Table 3. The percentage inhibition of α-amylase enzyme shown by AgNPs was higher as compared to the plant sample but lower than the standard acarbose.

Table 3
Comparison of percentage inhibition results shown by acarbose, plant, and AgNPs

Concentration (µg/ml)	Acarbose inhibition (%)	Plant extracts inhibition (%)	AgNPs inhibition (%)
100	60	22	54
200	74	38	58
300	76	44	64
400	82	50	76
500	86	56	80

3.5 TBARS assay

Figure 10 shows the concentration of MDA produced (in nmol) and AgNPs and the plant extract-treated group. The results of the AgNPs are significant as compared to the plant extract.

4 Discussion

Nanotechnology has got success in addressing many severe health care problems, food and feed, cosmetics, gene/drug delivery, mechanics, environment, and catalysis [24–29]. There are various applications of AgNPs e.g. as antimicrobial agents, anti-inflammatory agents, anti-cancer agents, and in wound healing processes [30–33].

In the present study; UV analysis was performed for confirmation of AgNPs synthesis. Optical absorption spectra are dependent on the shape and size of the AgNPs and are dominated by “surface plasmon resonance” that generally shifted to greater wavelengths with an increase in the particle size [34]. UV-visible spectroscopy showed a maximum absorption peak at 425 nm which conformed to the formation of AgNPs. The results of the present study are supported by [16] who reported the green synthesis of AgNPs by using *Calligonum polygonoides* crude extract.

Various concentrations (0.5-2 ml) of plant extract were used and absorbance was recorded in UV-Visible spectrophotometer at 425, 425, 430, and 430 nm. The Surface Plasmon Resonance bands became sharper by increasing plant extract concentration and appeared at 430 (absorbance 0.99982) at a lower concentration of 0.5 ml and 425 nm (absorbance 1.6) at higher concentration of 2 ml. The broadband at a lower concentration of the extract was mainly due to the formation of the anisotropic particles [35].

Different temperature conditions 25ºC, 50ºC, 75ºC, and 100ºC were used for AgNPs synthesis. Absorbance at 435, 430, 425, and 425 nm were recorded. At lower temperature, a 25ºC absorbance peak of 425 (absorbance 1.75) was observed which increase with an increase in temperature and a final absorbance peak of 435 nm (absorbance 2.401) was observed at 100ºC. Similar results were reported by [36].

In the present study; AgNPs were synthesized at different time intervals. Absorbance (1.279992) at 409 nm appeared after 5 minutes. This absorbance peak became sharp with the passage of time and a final 430 nm peak with the absorption of 2.1996 was recorded after twenty-four hours.

The formation of AgNPs was carried out at different pH. An almost straight line was observed at acidic pH values of 1–6 while with an increase of pH the sharp peaks 420, 425, and 430 nm were recorded in the pH range of 7–12. The synthesis of the AgNPs was repressed by acidic conditions and improved by basic conditions [35].

The presence of the different functional groups which are involved in the capping and reducing of AgNPs are conformed by FTIR analysis. The FTIR analysis showed different peaks which correspond to the different functional groups. The smaller sharp peaks at 3750 cm^{-1} indicate OH stretching of alcohols and phenols, and peaks near 3400 cm^{-1} represent the presence of alkyne CH bond and primary amines. This suggests the interaction of plant extract phenolic compounds with that AgNPs [37]. Another broad peak around 1600 cm^{-1} represents the amide stretching bond that might be associated with proteins that are involved in silver ion reduction. These findings confirm the occurrence of organic molecules on the surface of the synthesized AgNPs as mentioned in the findings of [2].

For structural analysis, the XRD patterns of the prepared materials were studied. Four strong Bragg reflections at 38°, 44°, 64°, and 78° resemble the planes of (1 1 1), (2 0 0), (2 2 0), and (3 1 1) respectively which can be indexed according to the face of the face-centered cubic crystal structure of silver. The calculated average crystallite of the AgNPs is 11.45 nm for four major peaks 38°, 44° 64°, and 78° of XRD. Similar results were also reported by [16, 38].

Morphology and distribution of AgNPs were examined by SEM. SEM demonstrated the average size of the synthesized nanoparticles in the range of 20 nm. Some nanoparticles of great size might be due to aggregation of smaller particles that happens during the drying process in an oven. The present results indicated that AgNPs have sphere-shaped Similar size ranges shape of AgNPs have been reported by [16].

The AgNPs synthesis was also confirmed by EDX analysis. EDX presented a discrete peak for elemental Ag. However, some of the other impurities including Na, Mg, and O were also observed. The occurrence of impurities may be due to matrix leftover. It might be from the glass support that was used for sample mounting just before the EDX analysis. This greater percentage of Ag, as examined by elemental investigation established that the particles were mostly composed of Ag [39].

Similar results are obtained about the antifungal activity. The synthesized AgNPs showed good antifungal activity by inhibiting *A. niger* and *A. flavus* fungal strains. The exact antifungal mechanism is not fully understood, but it is understood that they cause permeability of the fungal membrane and causes their inactivity [40].

The mechanism by which AgNPs exhibit antibacterial activity is not fully known yet. Many reports are there suggest that AgNPs adhere to the surface of the cell membrane of the bacteria and thus result in the disruption of their functional inactivity [41]. Earlier reports of [40] demonstrated the antibacterial activity of the AgNPs dependent on the size of the NPs. It is evident that smaller NPs having greater surface area shows the greater bactericidal activity as compared to larger NPs. It is also suggested that the smaller NPs not only attach to the cell membrane of the bacteria but also get penetration inside the cells and resulting in cell death. Our results demonstrated good antibacterial activity against tested pathogens which is similar to [42].

DPPH is synthetic-free radicals that are used to assess the antioxidant activity of desired compounds and molecules. In the current investigation, the DPPH radical scavenging activity of green synthesized AgNPs was explored in comparison with the standard (ascorbic acid) and plant extract. AgNPs showed good activity in comparison with the extract. Our results are similar to the findings of [16]. The antioxidant activity of the AgNPs is probably due to its electron-donating capability with which it gets stabilizes the free radicals [43–45].

ABTS is also free radicals that are used in antioxidant assays. The antioxidant activity of the synthesized AgNPs depends upon concentration. Our results are in accordance with [46–48].

Hydrogen peroxide is an unstable inorganic species [49] and due to its instability characteristic, it acts as a free radical. In the current study; AgNPs were used as a scavenger for these free radicals. The NPs showed good concentration-dependent antioxidant activity. The results are by the reports got earlier [50, 51].

In the small intestine, two principal enzymes are present for polysaccharides' metabolism. These are termed α-amylase and β-glucosidase. These enzymes convert the consumed polysaccharides to monosaccharides. The action of enzymes on polysaccharides generally results in an increased postprandial blood glucose quantity. This is due to the captivation of glucose from polysaccharides in the small intestine [52]. Those medications having an inhibition-like action on these enzymes might control the increase in post-prandial blood glucose levels. In the market, numerous drugs are present to be used for this purpose. The current results of our work demonstrated significant α-amylase activity that was obtained from the synthesized AgNPs. The extract activity was not significant as compared to the AgNPs which shows their good enzyme inhibitory action [16].

LPO (Lipid peroxidation) is a key feature of MDA as lipid peroxidation can result in increased oxidative stress [53]. The increased MDA and TBARS levels reflect higher lipid peroxidation. Our results showed the ability of AgNPs to inhibit LPO significantly.

5 Conclusions

The current study concluded that *V. anagallis-aquatica* possesses the ability to synthesize AgNPs cheaply. UV-visible spectroscopy demonstrated that the AgNPs synthesis is directly proportional to the

extract concentration and vice versa. Various phytochemicals shown by FTIR stay responsible for the green synthesis of AgNPs. The crystalline nature and average size of 11.45 nm are calculated using XRD analysis. The size of AgNPs confirmed by SEM was 20 nm. EDX analysis showed the presence of various impurities including Na, Mg, O, etc. Good antimicrobial, antioxidant, and sugar reducing activity was possessed by the synthesized AgNPs. MDA levels were reduced by the green synthesized AgNPs as compared to the plant extract.

Declarations

Acknowledgments

The author wishes to thank the Higher Education Commission of Pakistan (HEC-PAK) for financial support of project No: 20-5082/NRPU/R&D/HEC.

Conflict of Interest

The authors do not have any conflict of interest regarding this article and its publication.

References

1. M.A.M.M. Barkat, Harshita, S. Beg, M.J. Naim, F.H. Pottoo, S.P. Singh, F.J. Ahmad, Current Progress in Synthesis, Characterization and Applications of Silver Nanoparticles: Precepts and Prospects, Recent Pat Antiinfect Drug Discov. **13**(1), 53-69 (2018).
2. X. Zhang, Z. Liu, W. Shen, S. Gurunathan, Silver Nanoparticles: Synthesis, Characterization, Properties, Applications, and Therapeutic Approaches, Int J Mol Sci. . **17** (9), 1534 (2016).
3. I. Sondi, B. Salopek-Sondi, Silver nanoparticles as antimicrobial agent: a case study on E. coli as a model for Gram-negative bacteria, Journal of Colloid and Interface Science. **275** (1), 177-182 (2004).
4. M. Goudarzi, N. Mir, M. Mousavi-Kamazani, S. Bagheri, M. Salavati-Niasari, Biosynthesis and characterization of silver nanoparticles prepared from two novel natural precursors by facile thermal decomposition methods, Scientific Reports. **6**32539 (2016).
5. H.M.M. Ibrahim, Green synthesis and characterization of silver nanoparticles using banana peel extract and their antimicrobial activity against representative microorganisms, Journal of Radiation Research and Applied Sciences. **8**(3), 265-275 (2015).
6. V.G. Duschak, Synthetic Biology: Computational Modeling Bridging the Gap between In Vitro and In Vivo Reactions, Current Synthetic and Systems Biology. **3**(3), 2332-0737 (2015).
7. C.A. Ottoni, M.F. Simões, S. Fernandes, J.G.D. dos Santos, E.S. da Silva, R.F.B. de Souza, A.E. Maiorano, Screening of filamentous fungi for antimicrobial silver nanoparticles synthesis, AMB Express. **7**(31), 1-10 (2017).
8. F.I. Staquicini, M.G. Ozawa, C.A. Moya, W.H.P. Driessen, E.M. Barbu, H. Nishimori, S. Soghomonyan, L.G. Flores, 2nd, X. Liang, V. Paolillo, M.M. Alauddin, J.P. Basilion, F.B. Furnari, O. Bogler, F.F. Lang,

K.D. Aldape, G.N. Fuller, M. Höök, J.G. Gelovani, R.L. Sidman, W.K. Cavenee, R. Pasqualini, W. Arap, Systemic combinatorial peptide selection yields a non-canonical iron-mimicry mechanism for targeting tumors in a mouse model of human glioblastoma, J Clin Invest. **121**(1), 161-173 (2011).

9. D.H. Jo, J.H. Kim, T.G. Lee, J.H. Kim, Size, surface charge, and shape determine therapeutic effects of nanoparticles on brain and retinal diseases, Nanomedicine. **11**(7), 1603-11 (2015).
10. X. Duan, Y. Li, Physicochemical characteristics of nanoparticles affect circulation, biodistribution, cellular internalization, and trafficking, Small. **9**(9-10), 1521-32 (2013).
11. E. Abbasi, M. Milani, S.F. Aval, M. Kouhi, A. Akbarzadeh, H.T. Nasrabadi, P. Nikasa, S.W. Joo, Y. Hanifehpour, K. Nejati-Koshki, M. Samiei, Silver nanoparticles: Synthesis methods, bio-applications and properties, Crit Rev Microbiol. **42**(2), 173-80 (2016).
12. M. Chen, Y. Feng, X. Wang, T. Li, J. Zhang, D. Qian, Silver Nanoparticles Capped by Oleylamine: Formation, Growth, and Self-Organization, Langmuir **23**(10), 5296-5304 (2007).
13. A. Ahmad, P. Mukherjee, S. Senapati, D. Mandal, M.I. Khan, R. Kumar, M. Sastry, Extracellular biosynthesis of silver nanoparticles using the fungus Fusarium oxysporum, Colloids and Surfaces B: Biointerfaces. **28**(4), 313-318 (2003).
14. P. Rauwel, S. Küünal, S. Ferdov, E. Rauwel, A Review on the Green Synthesis of Silver Nanoparticles and Their Morphologies Studied via TEM, Advances in Materials Science and Engineering **2015** 1-9 (2015).
15. R. Geethalakshmi, D.V.L. Sarada, Gold and silver nanoparticles from Trianthema decandra: synthesis, characterization, and antimicrobial properties, Int J Nanomedicine. **7** 5375-5384 (2012).
16. N. Sher, M. Ahmed, N. Mushtaq, R.A. Khan, Calligonum polygonoides reduced nanosilver: A new generation of nanoproduct for medical applications, European Journal of Integrative Medicine. **33**(2020), 101042 (2020).
17. D.G. Baker, Antimicrobial susceptibility testing of Francisella tularensis with a modified Mueller-Hinton broth, J of Clinical Microbiology **22**(2), 212-215 (1985).
18. J.P. Ruparelia, A.K. Chatterjee, S.P. Duttagupta, S. Mukherji, Strain specificity in antimicrobial activity of silver and copper nanoparticles, Acta Biomater. **4**(3), 707-16 (2008).
19. W. Brand-Williams, M.E. Cuvelier, C. Berset, Use of a free radical method to evaluate antioxidant activity, Food Sci Technol-LWT. **28**(1), 25-30 (1995).
20. S. Mathew, T.E. Abraham, In vitro antioxidant activity and scavenging effects of Cinnamomum verum leaf extract assayed by different methodologies, Food Chem Toxicol. **44**(2), 198-206 (2006).
21. E. Pick, D. Mizel, Rapid microassays for the measurement of superoxide and hydrogen peroxide production by macrophages in culture using an automatic enzyme immunoassay reader, J Immunol Methods. **46**(2), 211-26 (1981).
22. C.P. Malik, M.B. Singh, Plant Enzymology and Histoenzymology, Kalyani publishers, New Delhi. 278 (1981).

23. H. Ohkawa, N. Ohishi, K. Yagi, Assay for lipid peroxides in animal tissues by thiobarbituric acid reaction, Anal Biochem. **95**(2), 351-8 (1979).
24. A. Bouvree, J. Feller, M. Castro, Y. Grohens, M. Rinaudo, Conductive Polymer nano-bioComposites (CPC): Chitosan-carbon nanoparticle a good candidate to design polar vapour sensors, Sensors & Actuators: B. Chemical **138** (1), 138-14 (2009).
25. L.S. Nair, C.T. Laurencin, Silver Nanoparticles: Synthesis and Therapeutic Applications, Journal of Biomedical Nanotechnology. **3**(4), 301-316 (2007).
26. R.M. Ganesan, H. Gurumallesh Prabu, Synthesis of gold nanoparticles using herbal Acorus calamus rhizome extract and coating on cotton fabric for antibacterial and UV blocking applications, Arabian Journal of Chemistry. **12**(8), 2166-2174 (2019).
27. P. Espitia, N. Soares, J. Coimbra, N. Andrade, R. Cruz, E. Medeiros, Zinc Oxide Nanoparticles: Synthesis, Antimicrobial Activity and Food Packaging Applications, Food and Bioprocess Technology. **5**(5), 1447–1464 (2012).
28. V. Sharma, R. Yngard, Y. Lin, Silver nanoparticles: green synthesis and their antimicrobial activities, Advances in colloid and interface science. **145**(1-2), 83-96 (2008).
29. S.H. Othman, Bio-nanocomposite Materials for Food Packaging Applications: Types of Biopolymer and Nano-sized Filler, Ital. Oral Surg. **2** 296-303 (2014).
30. S.J. Jacob, J.S. Finub, A. Narayanan, Synthesis of silver nanoparticles using Piper longum leaf extracts and its cytotoxic activity against Hep-2 cell line, Colloids Surf B Biointerfaces. **91**212-4 (2012).
31. V. Dhand, L. Soumya, S. Bharadwaj, S. Chakra, D. Bhatt, B. Sreedhar, Green synthesis of silver nanoparticles using Coffea arabica seed extract and its antibacterial activity, Mater Sci Eng C Mater Biol Appl. **58**36-43 (2016).
32. D. Jain, H.K. Daima, S. Kachhwaha, S.L. Kothari, Synthesis of plant-mediated silver nanoparticles using papaya fruit extract and evaluation of their anti microbial activities Digest Journal of Nanomaterials and Biostructures **4**(3), 557 - 563 (2009).
33. A. Nabikhan, K. Kandasamy, A. Raj, N.M. Alikunhi, Synthesis of antimicrobial silver nanoparticles by callus and leaf extracts from saltmarsh plant, Sesuvium portulacastrum L, Colloids Surf B Biointerfaces. **79**(2), 488-93 (2010).
34. P.L. Nadworny, J. Wang, E.E. Tredget, R.E. Burrell, Anti-inflammatory activity of nanocrystalline silver in a porcine contact dermatitis model, Nanomedicine. **4**(3), 241-51 (2008).
35. M. Amin, F. Anwar, M.R. Janjua, M.A. Iqbal, U. Rashid, Green synthesis of silver nanoparticles through reduction with Solanum xanthocarpum L. berry extract: characterization, antimicrobial and urease inhibitory activities against Helicobacter pylori, Int J Mol Sci. **13**(8), 9923-41 (2012).
36. I. Pastoriza-Santos, L.M. Liz-Marzan, Formation of PVP-protected metal nanoparticles in DMF, Langmuir. **18**(7), 2888-2894 (2002).
37. M. Rai, A.Y.A. Gade, Silver nanoparticles as a new generation of antimicrobials, Biotechnology Advances. **27** (1), 76-83 (2009).

38. K. Jemal, B.V. Sandeep, S. Pola, Synthesis, Characterization, and Evaluation of the Antibacterial Activity of Allophylus serratus Leaf and Leaf Derived Callus Extracts Mediated Silver Nanoparticles Journal of Nanomaterials **2017**(3), 1-11 (2017).
39. M. Parveen, F. Ahmad, A.M. Malla, S. Azaz, Microwave-assisted green synthesis of silver nanoparticles from Fraxinus excelsior leaf extract and its antioxidant assay, Applied nanoscience. **6**(2), 267-276 (2016).
40. J. López-Miranda, Luis, M. Vázquez, N. Fletes, R. Esparza, G. Rosas, Biosynthesis of silver nanoparticles using a Tamarix gallica leaf extract and their antibacterial activity, Materials Letters. **176** ( ), 285-289 (2016).
41. A. Nasrollahi, K. Pourshamsian, P. Mansourkiaee, Antifungal activity of silver nanoparticles on some of fungi, Int.J.Nano.Dim. **1**(3), 233-239 (2011).
42. R.T. Narendhirakannan, S. Subramanian, M. Kandaswamy, Biochemical evaluation of antidiabetogenic properties of some commonly used indian plants on streptozotocin-induced diabetes in experimental rats, Clinical and experimental pharmacology and physiology. **33**(12), 1150-1157 (2006).
43. D.J. Mabberley, D.J. Mabberley, *Mabberley's plant-book : a portable dictionary of plants, their classifications, and uses*. 2017.
44. R. Balamurugan, V. Duraipandiyan, S. Ignacimuthu, Antidiabetic activity of g-sitosterol isolated from Lippia nodiflora L. in streptozotocin induced diabetic rats, Eur J Pharmacol. **667** (1-3), 410-18 (2011).
45. S. Pradeepa, S. Subramanian, V. Kaviyarasan, Biochemical evaluation of antidiabetic properties of Pithecellobium dulce fruits studied in streptozotocin induced experimental diabetic rats, International Journal of Herbal Medicine **1**(4), 21-28 (2013).
46. J. Mohammadi, P.R. Naik, Evaluation of hypoglycemic effect of Morus alba in an animal model, Indian J Pharmacol. **40**(1), 15-8 (2008).
47. A. Dina, C. Nassima, B. Meriem, A. Karima, L. Hakima, B. Hania, D. Nadjet, A. Djebbar, Antioxidant capacity and phenol content of selected Algerian medicinal plants, Food Chemistry. **112**(2), 303-309 (2009).
48. A. Djeridane, M. Yousfı, B. Nadjemi, D. Boutassouna, P. Stocker, N. Vidal, Antioxidant activity of some Algerian medicinal plants extracts containing phenolic compounds, Food Chemistry. **97**(4), 654-660 (2006).
49. G.L. Miller, Use of Dinitrosalicylic Acid Reagent for Determination of Reducing Sugar, Anal. Chem. **31**(3), 426-428 (1959).
50. A. Aboonabi, A. Rahmat, F. Othmanb, Antioxidant effect of pomegranate against streptozotocin-nicotinamide generated oxidative stress induced diabetic rats, Toxicol Rep. **1** 915-922 (2014).
51. Q. You, F. Chen, X. Wang, P.G. Luo, Y. Jiang, Inhibitory effects of muscadine anthocyanins on α-glucosidase and pancreatic lipase activities, J Agric Food Chem. **59**(17), 9506-11 (2011).
52. P. Diouf, A. Merlin, D. Perrin, Antioxidant properties of wood extracts and colour stability of woods, Ann. For. Sci. () **63** (5), 525-534 (2006).

53. A. Eidi, P. Mortazavi, M. Bazargan, J. Zaringhalam, Hepatoprotective activity of cinnamon ethanolic extract against CCl4-induced liver injury in rats, EXCLI J **11**495-507 (2012).

Figures

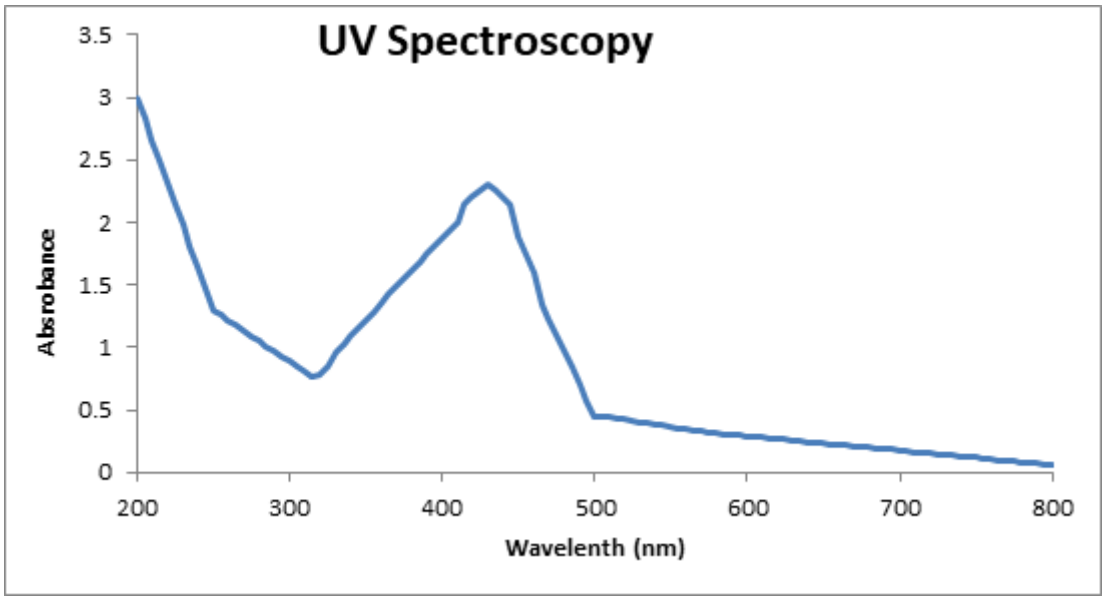

Figure 1

The UV-vis absorption spectrum of AgNPs. *V. anagallis-aquatica* Volume: 1 ml; time: 24 hours; temperature: 25 ºC; pH: 10

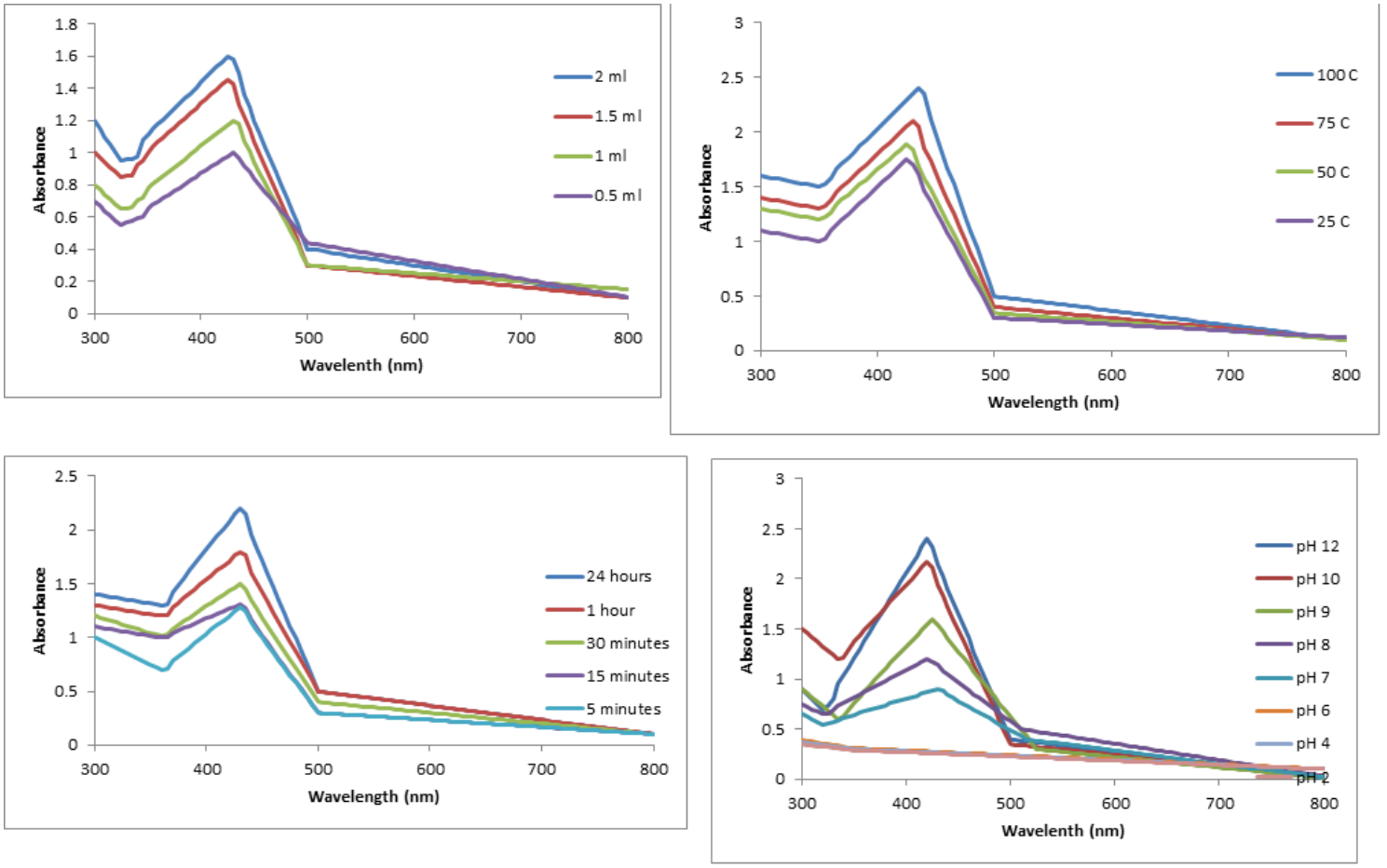

Figure 2

a The UV-vis absorption spectrum with different volumes of *V. anagallis-aquatica*. Time: 24 hours; Temperature: 25 ºC; pH: 10

b The UV-vis absorption spectrum with different temperatures. *V. anagallis-aquatica* volume: 1 ml; time: 24 hours; pH: 10

c The UV-vis absorption spectrum of AgNPs at different times. *V. anagallis-aquatica* volume: 1 ml; temperature: 25 ºC; pH: 10

d The UV-vis absorption spectrum of AgNPs at acidic and basic conditions. *V. anagallis-aquatica* volume: 1 ml; temperature: 25 ºC; time 24 hours

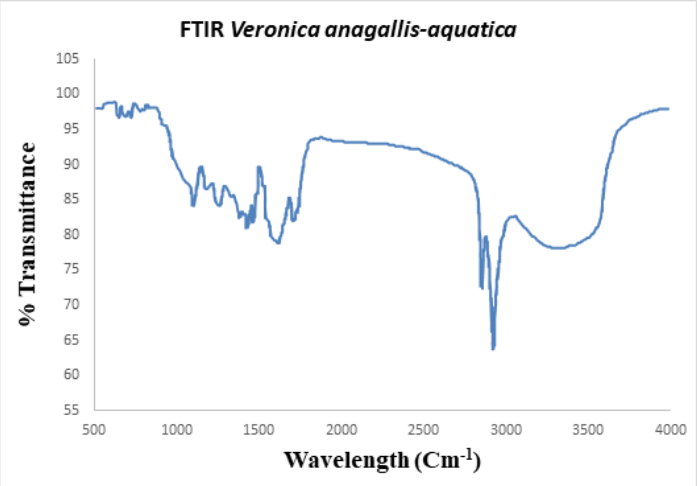

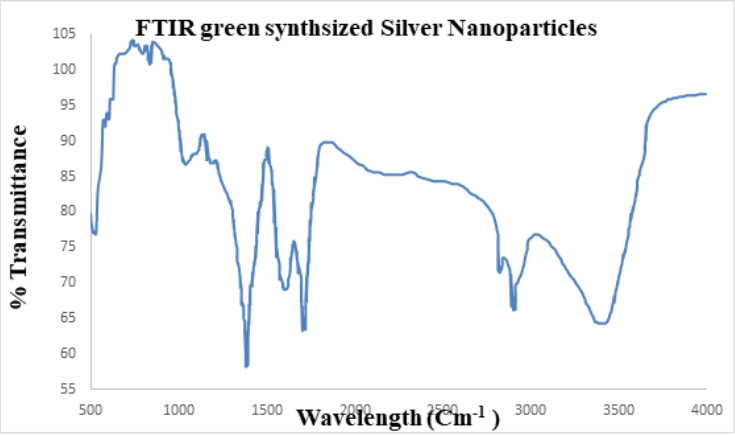

Figure 3

a FTIR spectrum of *V. anagallis-aquatica* plant extract

b FTIR spectrum of *V. anagallis-aquatica* green synthesized AgNPs indicates different functional groups

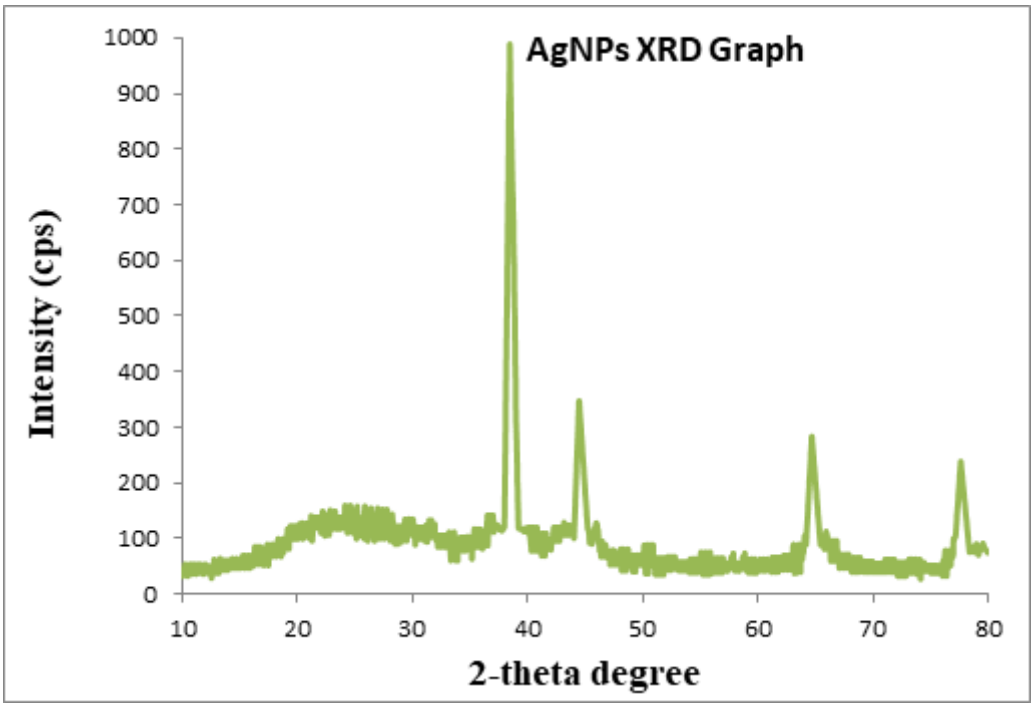

Figure 4

XRD analysis of AgNPs AgNPs.

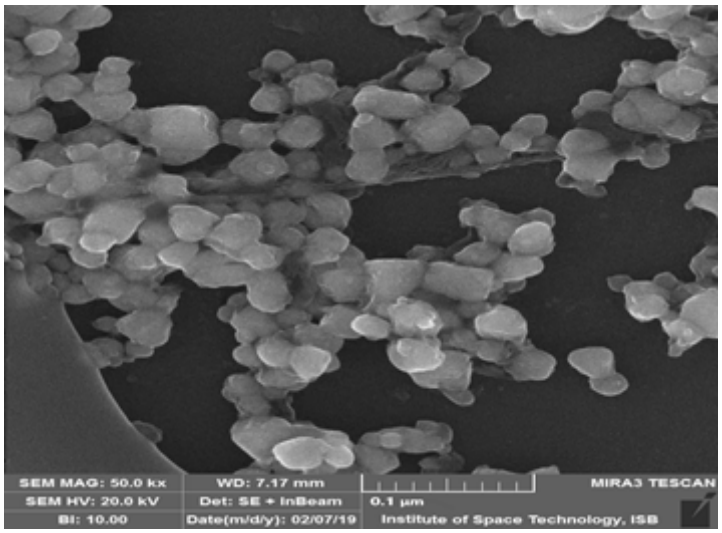

Figure 5

SEM analysis of AgNPs.

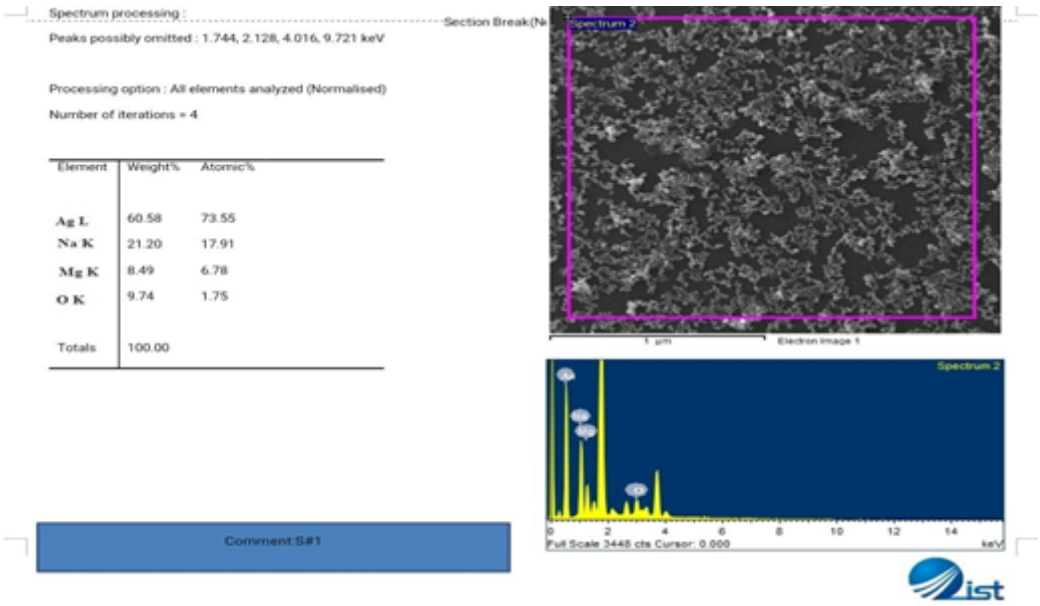

Figure 6

EDX analysis graph

Figure 7

Antifungal results .activity of AgNPs and plant extract.

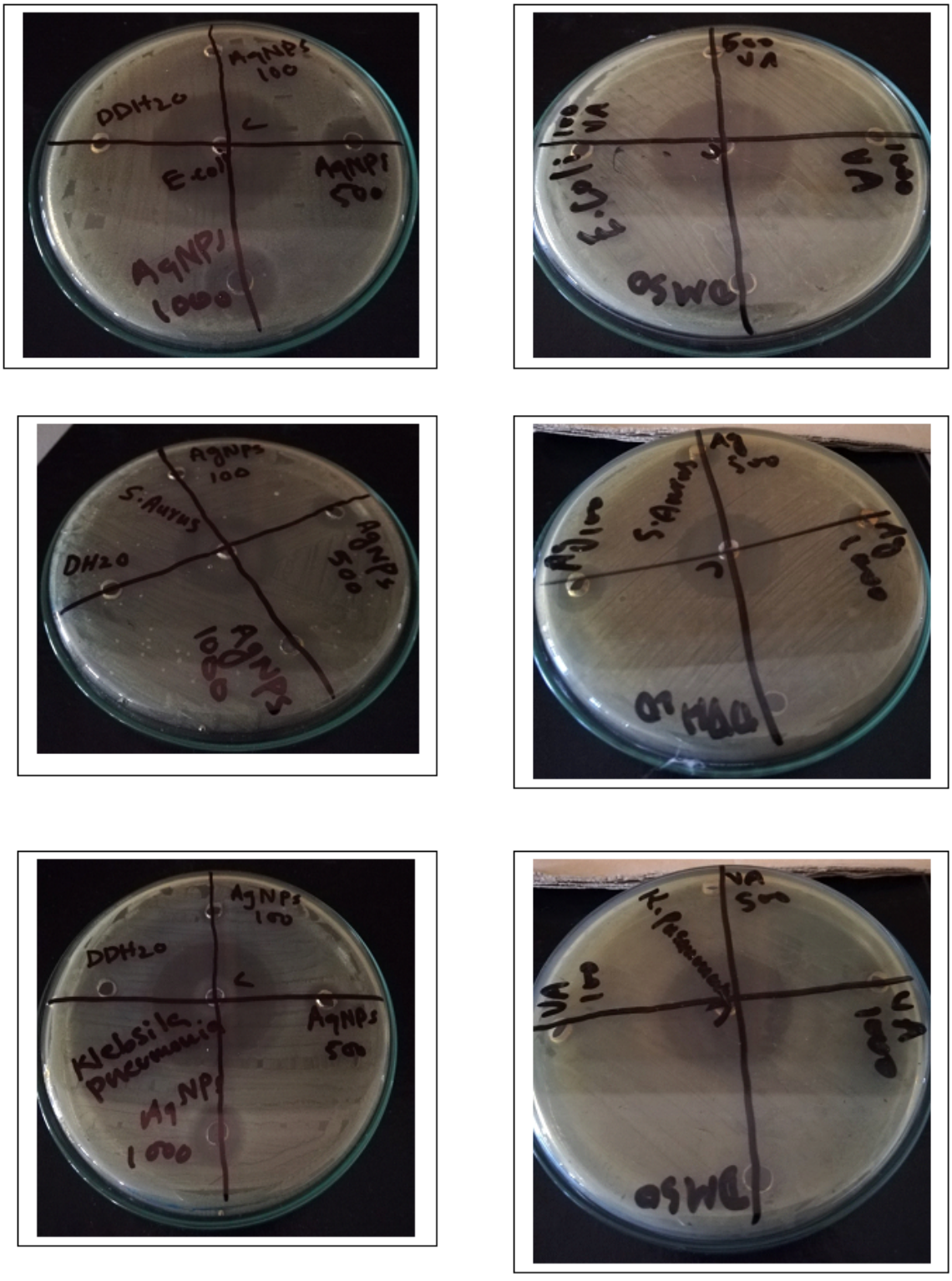

Figure 8

Antibacterial activity of AgNPs and plant extract.

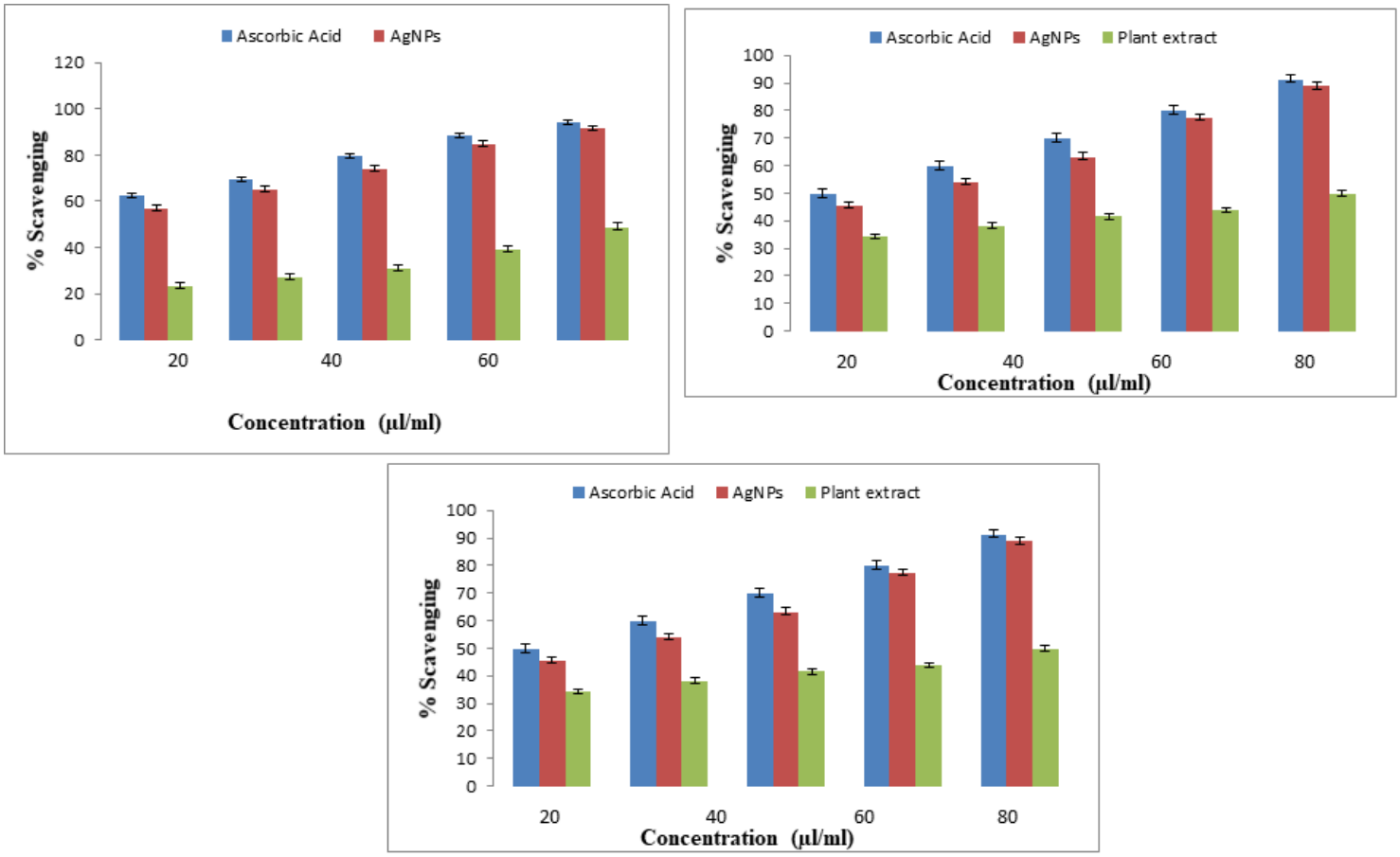

Figure 9

a DPPH scavenging Assay of AgNPs and plant extract.

b ABTS scavenging assay of AgNPs and plant extract.

c Hydrogen peroxide scavenging assay of AgNPs and plant extract.

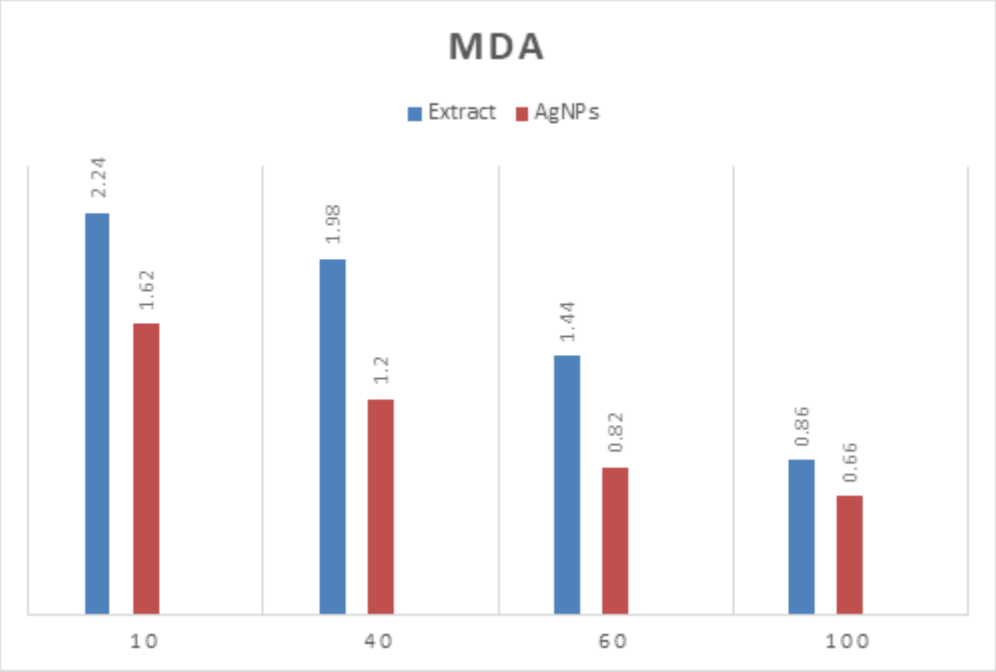

Figure 10

MDA (nmol/mg protein) in plant extract and AgNPs treated groups.